Accuracy and Coverage of Temperature Data Derived from the IR Radiometer on the NOAA 2 Satellite

ROBERT JASTROW AND MILTON HALEM

Goddard Institute for Space Studies, NASA, New York, N. Y. 10025

23 May 1973 and 3 July 1973

1. Introduction

The Vertical Temperature Profile Radiometer (VTPR) on the NOAA 2 satellite has been returning useful temperature data since shortly after the time of its launch on 15 October 1972. The principal purpose of this instrument is the provision of daily temperature soundings on an operational basis over the oceans, as an addition to the primarily ground-based global data network used by the National Weather Service. We would like to report on results obtained with VTPR data in a non-operational research project, with the eventual aim of determining the potential value of satellite temperature observations as a separate data base independent of conventional observations. The work described in the present report still relies on conventional observations for assistance in the inversions, the cloud-filtering procedure, and the minimization of systematic errors.

The specific goal of the project is the complete determination of global atmospheric states or Initial State Parameters (ISP's)—including wind and pressure as well as temperature—from VTPR radiances alone. The project involves three stages. The first stage, which is the subject of the present report, is concerned with the accuracy, frequency and global distribution of the VTPR-derived temperature profiles. The second stage consists in the assimilation of the VTPR data to produce ISP's. The third stage will investigate the range and accuracy of global forecasts based on these satellite-derived ISP's.

2. Limitation on simulation studies

Simulation studies (Jastrow and Halem, 1970) indicate that ISP's of good quality should be obtainable from the sounding radiometers planned for the First GARP Global Experiment in 1977. However, the simulation results contain two major uncertainties. The first uncertainty relates to the fact that all simulation studies minimize the shock of direct data assimilation, since the simulated "data" are obtained from the same model that is used for data assimilation and verification. This fact tends to make the simulation study results more favorable than results obtained with real data of the same quality. The follow-on studies referred to above will yield information on the size of this effect.

The second uncertainty in the simulation results relates to the accuracy of the data yielded by the actual sounder in an operational mode and to the geographical distribution and frequency of the soundings, which may not match the assumptions on which the simulation studies were based. The assumptions involved are 1) an rms accuracy of 1C, 2) a uniform global coverage, and 3) a frequency of usable soundings corresponding to two profiles per grid point per day on a 400-km grid, or a global total of 6000 temperature profiles per day. The operational sounder may fail to satisfy these requirements either because of failure of the radiometer to meet specifications, or because practical difficulties—especially in the elimination of cloud effects—interfere with the theoretical programs for the conversion of the radiance data into temperature profiles. Here we are concerned with the questions of accuracy, coverage and frequency of usable soundings.

3. Temperature inversion technique

The technique employed in the analysis uses the basic inversion scheme developed by Chahine (1968) with subsequent modifications by Smith (1970) and Hogan and Grossman (1972). The initial guess employed in the inversions is taken from the NMC temperature analyses for the Northern Hemisphere above 18° latitude, and the Stackpole-Flattery global analysis for other latitudes. In the studies of the accuracy of the cloud-filtering technique, the first guess for each inversion was taken from the current temperature analysis. In the experiments designed to test the accuracy of the satellite-derived temperature in which the satellite data would be used for numerical prediction, the first guess was a 12-hr forecast generated by the Goddard Institute for Space Studies (GISS) model from initial conditions provided by the NMC analysis from the previous synoptic time. In these latter experiments, the satellite-derived temperatures and radiosonde profiles were averaged over atmospheric layers 110 mb thick. This thickness was chosen to match the vertical resolution in the GISS 9-level model used for data assimilation and forecast studies based on VTPR data.

4. Techniques for eliminating cloud effects

With respect to accuracy, the principal problem in the analysis of the VTPR data is the presence of an unknown amount of cloud cover in the field-of-view of the vast majority of the soundings. If cloud effects are not removed from the soundings, the rms temperature errors, calculated by comparison with co-located radiosonde observations, average ~5C. This error is somewhat smaller than the mean difference in the temperature fields of two uncorrelated flows, which is ~7C, but is not small enough to make the VTPR data a useful adjunct to the existing data base in meteorology. Therefore, the primary requirement in the processing of the sounding data, after the development of the basic inversion program, becomes the development of an effective scheme for removing cloud effects from the soundings. The cloud-filtering problem has been considered by Smith (1967) and Chahine (1970) who have developed somewhat different methods. The method employed below is similar to that described by Chahine.

The effect of clouds on the temperature profiles depends on the fraction η of cloud cover in the field-of-view of the sounder, and on the height or pressure P_c of the cloud tops. In the present procedure for processing the VTPR data, P_c is calculated first and η second.

The method employed for the determination of P_c was suggested by Chahine (1970). It rests on the observation that above the cloud-top level all soundings should yield approximately the same profile, but below this level the profiles should diverge; that is, all profiles in a given region meet at a pressure which is the approximate cloud-top pressure P_c (Fig. 1). This qualitative property of the soundings in the vicinity of a given point has been translated into a simple computational algorithm by Ungar (private communication) for determining P_c, in which the "hottest" and "coldest" soundings in a group are selected, i.e., the pair of soundings with the highest and lowest radiances, respectively, in the window channel. This pair of soundings is then inverted assuming no clouds. The resultant profiles give the maximum spread in temperature below the clouds in that region, and, therefore, the highest accuracy in the determination of P_c.

With P_c determined, the next step is the determination of η. This is not possible with the information provided by the radiances alone, because any given set of observed radiances can be inverted to obtain a wide range of temperature profiles, corresponding to various choices of η between 0 and 1. This may be seen from the expression

$$R^{\nu}_{\text{observed}} = (1-\eta)R^{\nu}_{\text{clear}} + \eta R^{\nu}_{\text{cloudy}}, \qquad (1)$$

where R^{ν}_{clear} is the radiance in the νth channel in the absence of clouds, and R^{ν}_{cloudy} the radiance in the νth channel assuming a cloud layer at height P_c. For a particular value of η, (1) may be solved for the clear-column radiances, R^{ν}_{clear}. This process can be carried out for any value of η between 0 and 1.

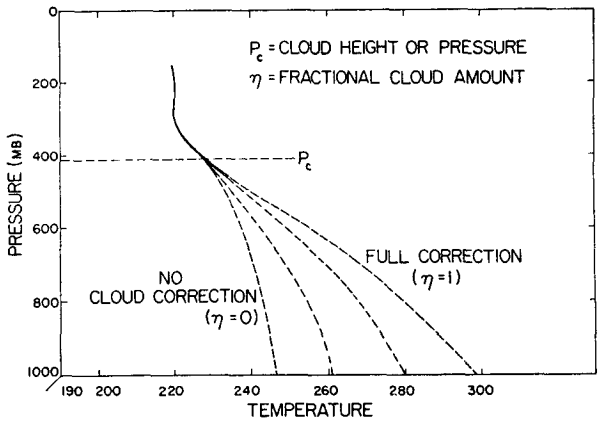

FIG. 1. The curves represent four distinct temperature profiles, all derived from the same set of observed radiances, but with different values assumed for η, the cloud fraction. The graph illustrates the indeterminacy introduced into the temperature-inversion problem by the presence of clouds in the field-of-view of the sounder. Abscissa units are °K.

The result is a family of curves, $T(P,\eta)$, schematically shown in Fig. 1. All four profiles in Fig. 1 are possible deductions from the same set of observed radiances. It is clear that because of the presence of clouds, an essential indeterminacy exists in the problem of inverting a set of observed radiances to find a temperature profile. The indeterminacy can only be removed if additional information is provided to fix the value of η. Fig. 1 suggests that a measurement of the surface temperature T_s would be a desirable form of input for fixing η, because the spread in the profiles, calculated for various values of η, is largest at the surface. Therefore, a specification of T_s should determine the value of η with maximum accuracy.

The procedure is implemented by performing the inversion for several values of η, and finding by interpolation the value of η that produces a temperature profile whose surface value agrees with the observed T_s. This η-interpolation method effectively anchors the entire profile to the specified value of T_s.

Several sources of information regarding T_s are available to make the proposed method useful in practice. In the Northern Hemisphere, surface stations and ship reports provide data twice daily. In the Southern Hemisphere, sea-surface temperature measurements are sparser but climatology provides values with a dispersion of a few degrees that may be good enough to be useful. Sea-surface temperature measurements from the scanning radiometer (SR) on NOAA 2 are expected to become operational shortly, and should provide global coverage for T_s with a precision of 1C. At the present time, SR data appear to be yielding sea-surface temperatures with an rms error of ~1.2C, as judged by comparison with available ground-truth

analyses in the shipping lanes of the Northern Hemisphere (Brower, personal communication). In the present study the NMC surface analyses were used north of 18N, and the Stackpole-Flattery global surface analyses south of 18N.

5. Basis for judging the accuracy of the temperature profiles

The effectiveness of the cloud-elimination technique was tested by comparisons with the global network of radiosonde stations included in the daily list of station reports collected by NOAA. The list includes approximately 600 station reports for 0000 and 1200 GMT each day. The test period began 9 December and ended 24 December. The complete file of approximately 2.5 million VTPR soundings for this 15-day period was searched and all soundings lying within ± 30 min of synoptic time were selected. The radiosonde observations and the selected soundings were stored on a disc and a second search was made for all soundings lying within a specified distance from all radiosonde stations (usually 100 km). The co-located points of observation are concentrated in swaths controlled by the sun-synchronous satellite orbit, which crosses the equator at 0900 and 2100 local time daily. A VTPR sounding was dropped from the comparison if the difference between the VTPR and radiosonde profiles exceeded 15C at one or more levels. Temperatures were then computed from all VTPR soundings in the vicinity of a given radiosonde station, and rms differences between the VTPR soundings and the radiosonde observations at standard pressure levels were listed and averaged.

In some early experiments, the individual soundings were converted to temperature profiles and the temperatures were then averaged, while in other experiments, the radiances were first averaged and temperatures were then computed from the averaged radiances. The results differed by no more than a few tenths of a degree in most cases. On the basis of these results, averaged radiances were used in the remainder of the experiment, since this procedure saves a substantial amount of computing time. The rms difference between the radiosonde observations and the co-located VTPR profiles for the 15-day period of the test was taken as the criterion for judging the accuracy of the satellite-derived temperatures.

In addition to computing the average rms error, the *algebraic* mean of the error at each standard pressure level was also computed. The table of algebraic mean errors was used as the basis for estimating the size of systematic effects. The systematic effects were exhibited most clearly when the table of algebraic mean errors was printed out separately for low-latitude (below 45N) and high-latitude stations. This table was the input to the tuning procedure described in the following section.

6. Tuning the temperature profiles

After cloud effects were reduced by application of the η-interpolation method, the mean error in the VTPR temperature profiles dropped from 5.60C to 2.24C. The error, as noted above, was determined by comparison with co-located radiosonde observations. At this point for the first time, systematic discrepancies appeared clearly in the comparisons between the VTPR data and the co-located radiosonde observations. These systematic errors were obscured by cloud contamination and were not apparent in the results prior to the filtering out of the cloud effects.

An example of such systematic errors is a uniformly negative error, i.e., soundings systematically colder than radiosonde observations, at low latitudes in the mid-troposphere between 200 and 800 mb, as seen in curve A of Fig. 3.

Presumably the major source of systematic errors lies in the atmospheric transmission functions used for the radiative transfer programs that convert radiances to temperatures. These transmission functions are computed from theoretical models of absorption band structure, and are uncertain by at least a few percent in each channel. However, systematic errors could also result from improper calibration of the sounder, or incorrectly specified filter functions for some channels, or residual errors in the determinations of P_c and η described above.

The systematic errors can be minimized conveniently by making small adjustments in the atmospheric transmission functions employed in the calculation. Assume

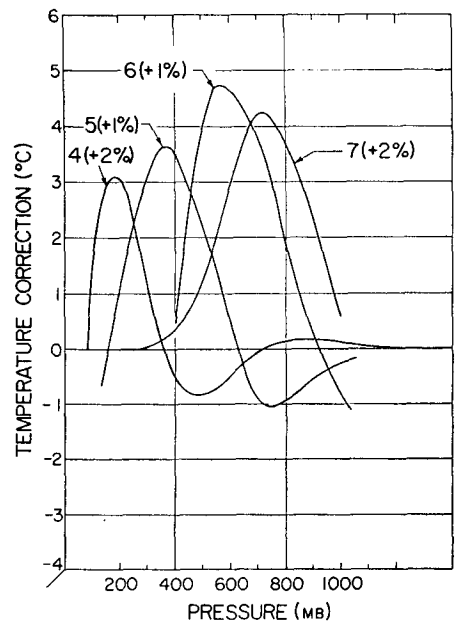

FIG. 2. Examples of curves of temperature variations produced by small changes in the mean absorption coefficient in each channel. These "tuning curves" were used to minimize systematic errors.

that the theoretically computed absorption coefficient, κ_ν, in the νth channel is to be adjusted by a fractional amount ϵ_ν. Then the adjusted optical thickness, τ_ν, is

$$\tau_\nu = (1+\epsilon_\nu)\int_z^\infty \kappa_\nu \rho dz.$$

Fig. 2 shows an example of the effect of small positive values of ϵ_ν, i.e., small increases in the mean absorption in selected channels of the VTPR sounder. Each curve in Fig. 2 was computed by changing the mean absorption in one channel, inverting the radiances using the modified absorprion coefficient, and comparing with the original profile. It is seen that the effect on the temperature profile is generally positive, as is to be expected, since an increase in the mean absorption in a given channel will decrease the amount of radiation emitted in that channel, and therefore the temperature must be increased in order to restore the radiation to the observed level of the radiance in that channel.

Fig. 2 shows that the temperature increase is concentrated at distinct pressure levels, depending on the channel chosen for the adjustment. This fact suggests that a superposition of corrections in the various channels, with properly chosen signs and magnitudes, can approximately compensate for any systematic error, provided the error varies smoothly with pressure.

For example, if the VTPR temperature is too low in the region between 200 and 800 mb, as noted above, an increase in the mean absorption coefficients in the channels that contribute to the radiation in this pressure interval will elevate the corresponding temperature in the profile deduced from the observed radiances. Curve A of Fig. 3 shows the systematic negative error between 200 and 800 mb, referred to above, and curve B shows the result of correcting the systematic error in the profile through adjustments of the mean absorption coefficient in each channel by the following amounts:

Channel (ν)	ϵ_ν
3	0.02
5	0.0075
6	0.0075
7	0.01

A general procedure can be developed for reducing systematic errors in any particular calendar period of the VTPR observations by first computing "tuning curves," analogous to the curves in Fig. 2, that give the differential response of the temperature profile to small changes in the mean absorption for each channel. The tuning curves are averaged over the calendar period to which the tuning procedure is to be applied. These curves, combined with the table of algebraic mean errors derived from the radiosonde comparisons, provide the basis for determining the set of ϵ_ν's that will minimize the systematic errors.

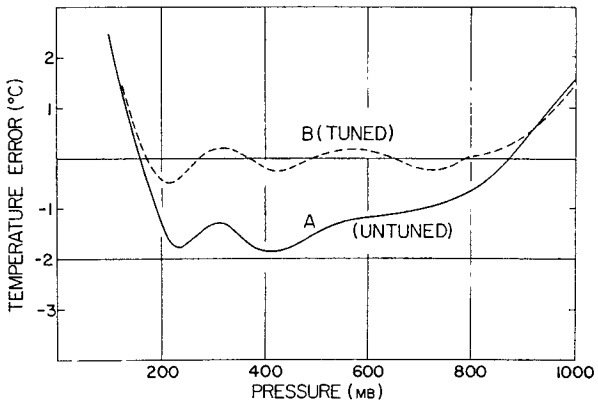

FIG. 3. Example of systematic errors in the VTPR-derived profiles. Curve A shows systematically cold retrievals (compared to radiosonde observations) obtained from VTPR soundings averaged over a two-day period in December. Curve B shows the errors in the same soundings after tuning, i.e., adjustment of mean absorption coefficients in channels 3–7 of the sounder.

This tuning method was applied to the radiance data for the test period 9–24 December. Tuning curves were first computed for a typical sounding, and the set of ϵ_ν's was then determined to minimize the systematic errors in the temperature profile for the period 9–12 December. This same set was used throughout the remainder of the 15-day period. The average rms error in the tuned profiles was 2.05C for the 15-day test period.

Fig. 4 shows the distribution of the temperature errors around the mean value. This graph represents comparisons between VTPR temperature profiles and 418 co-located radiosonde observations over the 15-day test period. These comparisons include every radiosonde

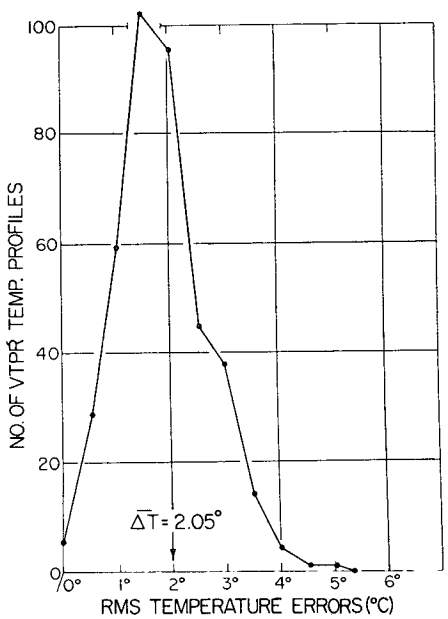

FIG. 4. The frequency distribution of temperature errors for profiles computed by the combination of cloud-filtering and tuning techniques.

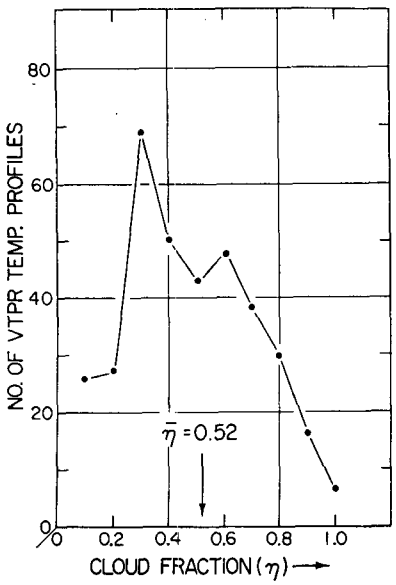

FIG. 5. Distribution of fractional cloud amounts computed by the automatic cloud-filtering techniques.

station in the test period that met the co-location requirement.

The value for the cloud fraction was also computed and stored for each temperature computation. The mean value of η was 0.52. The distribution of η values around the mean is shown in Fig. 5.

7. Effectiveness of the cloud-filtering technique

In view of the large magnitude of the cloud effects, it is important to evaluate the effectiveness of the technique employed here to correct the soundings for cloud-contamination. Fig. 6 shows the dependence of the rms temperature error on the fraction of cloud cover. The error is seen to be approximately independent of η between 0 and 0.8, but increases substantially between 0.9 and 1. This graph suggests that the cloud-filtering technique is effective for soundings in which the cloud cover is as much as 80%.

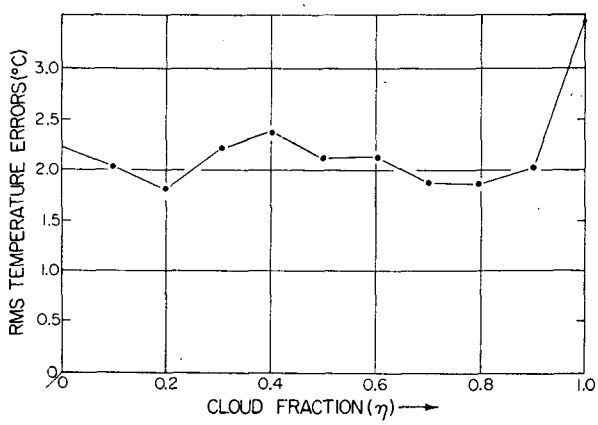

FIG. 6. Graph of rms temperature error vs η indicating that the cloud-filtering techniques are effective for cloud cover up to 80% of the field-of-view of the sounder.

8. Automatic tuning

Repeated re-tuning may improve the mean error obtained by using a single set of ϵ's for the entire test period, since the systematic errors may vary from day to day. However, frequent repetition of tuning is not feasible with the trial-and-error procedure described above, because it requires the better part of a day for the determination of one set of ϵ_ν's. An automatic tuning method has been developed which replaces this procedure by a systematic search of the ϵ_ν space, and requires only 20 min of 360/95 computing time for the tuning of the soundings to a 24-hr period of radiosonde observations. The method consists of: 1) computing tuning curves, automatically averaged over the time interval in which the tuning is to be performed; and 2) searching the space of the ϵ_ν's for a set of values which minimize the sum of the squares of the systematic errors (arithmetic mean differences between the VTPR profiles and co-located radiosonde profiles). The mean rms error computed for the 15-day test period from 9–24 December, with tuning repeated on the 9th, 13th, 17th and 21st, was 2.22C with a range from 1.85C to 2.72C. The co-location region in space-time is 50 km and $\pm$30 min.

It should be emphasized that this error estimate is based on a limited geographical distribution of radiosonde stations that happen to lie close to the subsatellite path of NOAA 2. The comparison stations are well distributed in latitude but not in longitude.

9. Global distribution and frequency of VTPR temperature soundings

The simulation studies on the assimulation of satellite-derived temperature profiles assume that these profiles are distributed uniformly over the globe and that each satellite provides soundings with a frequency corresponding to two usable profiles per grid point per day on a 400-km grid. The combination of the VTPR side-scan capability and the NOAA 2 orbit altitude is such that these requirements cannot be satisfied with the VTPR instrument, the principal inadequacy being a gap of roughly 2000 km at the equator in the coverage provided by successive orbital passes. The equatorial gap narrows with increasing latitude and disappears at roughly 50°. This effect reduces the frequency of soundinqs at the equator to 0.8 soundings per grid point per day, which constitutes the maximum theoretically attainable yield at the equator. At high latitudes, the coverage exceeds the nominal requirement of two profiles per grid point per day because of the overlap of

TABLE 1. Latitudinal distribution of usable VTPR temperature profiles.

Latitude (deg)	Yield (profiles per grid point per day)	Yield (percent of maximum attainable profiles per grid point per day)
80N	3.12	65
64N	2.52	86
48N	1.30	72
32N	0.90	55
16N	1.17	73
0	0.56	70
16S	0.89	56
32S	1.09	62
48S	1.55	86
64S	2.96	100
80S	2.92	61

successive orbits at the top of each pass. Here the theoretically attainable yield is approximately five soundings per grid point per day. The theoretically attainable yield, averaged over all latitudes and weighted by area, is 1.87 soundings per grid point per day.

Table 1 shows the latitudinal distribution in the yield of usable profiles per grid point per day obtained from the VTPR radiances by the techniques described here averaged over the December test period. The table also shows the yield of VTPR profiles expressed as a percentage of the maximum theoretically attainable yield for each latitude zone.

The average yield of VTPR profiles over all latitude zones, weighted by area, is 1.34 profiles per grid point per day, or roughly 4000 soundings per day, which is 72% of the maximum theoretically attainable yield. This result is less favorable than it appears to be, because in the computation of the average the large number of profiles in high latitudes obscures the inadequate coverage near the equator. If the high-latitude yield is arbitrarily cut off at an upper limit of two soundings per grid point per day in each latitude zone, the area-average yield is reduced to 1.19.

10. Conclusions

The results of this preliminary study indicate that temperature profiles with an rms error of 2.2C can be derived from the VTPR radiances on a continuing basis over periods of several weeks or longer. On some days the rms error is as low as 1.85C. On the basis of this analysis, the VTPR sounder is estimated to be capable of yielding profiles with an rms error of 1.5C if further improvements are introduced into the cloud-filtering and tuning techniques.

The yield of usable temperature profiles is roughly 70% of the maximum theoretically attainable yield with the VTPR side-scan capability and the orbit altitude of NOAA 2. The actual result is approximately 1.3 usable profiles per grid point per day for the December 1972 and April 1973 test periods. Improvements in the efficiency of the cloud-filtering technique may increase this value.

These results suggest that for the next generation of sounders (Nimbus F and Tiros N), with the 4.3 μm band added for better resolution near the ground (Smith, 1972), a global coverage with a temperature error of 1.5C or better and a yield of two temperature profiles per grid point per day per satellite is a realistic goal.

Acknowledgments. This research could not have been conducted without the active cooperation of the VTPR operational group in the National Environmental Satellite Service (NESS) of NOAA, under the direction of Dr. David Wark. The NESS VTPR staff provided software and operational support for regular transmission of VTPR data to GISS. On several occasions NESS also supplied additional VTPR data from the NESS archives for the conduct of new numerical experiments. This support from NESS was invaluable. Special thanks are due Messrs. H. McLure, B. Werbowetzki and F. Bittner in this connection.

The National Meteorological Center of NOAA also provided an invaluable service in furnishing both the daily operational NMC analyses and, as a special off-line operation, the Stackpole-Flattery global analyses. The global analyses, in particular, played an essential role in the present program. We are specially indebted to Lt. Col. H. O'Neil of NMC, who went to considerable effort on numerous occasions to ensure that NMC and global analyses were made available to GISS on relatively short notice.

Several members of the staffs of GISS and the Computer Sciences Corporation (CSC) made critically important contributions to the program.

We are also indebted to Dr. J. Hogan of GISS who adapted the Hogan/Grossman program to the special characteristics of the VTPR sounder, including the preparation of the CO_2 transmission functions for the 15-μm band. Dr. Hogan, Dr. S. Ungar and Mr. R. Karn of CSC were responsible for the establishment of the data-processing procedures and the initial testing of the inversion programs on VTPR data.

Finally we are deeply indebted to Messrs. D. Berman, D. Edelman, D. Chin, H. Carus, W. Budich and Dr. N. Rushfield, mathematical analysts and scientific programmers, in particular for their unusual degree of dedication in the prosecution of the project and their talented performance in the development of the programs and analytical procedures required for cloud filtering, tuning, data processing and documentation.

REFERENCES

Chahine, M. T., 1968: Determination of the temperature profile in an atmosphere from its outgoing radiance. *J. Opt. Soc. Amer.*, **58**, 1634–1637.

——, 1970: Inverse problems in radiative transfer: Determination of atmospheric parameters. *J. Atmos. Sci.*, **27**, 960–967.

Hogan, J., and K. Grossman, 1972: Tests of a procedure for inserting satellite radiance measurements into a numerical circulation model. *J. Atmos. Sci.*, **29**, 797–800.

Jastrow, R., and M. Halem, 1970: Simulation studies related to GARP. *Bull. Amer. Meteor. Soc.*, **51**, 490–513.

Smith, W. L., 1967: An improved method for calculating tropospheric temperature and moisture from satellite radiometer measurements. *Mon. Wea. Rev.*, **96**, 387–396.

——, 1970: Iterative solution of the radiative transfer equation for the temperature and absorbing gas profile of an atmosphere. *Appl. Opt.*, **9**, 1993–1999.

——, 1972: Satellite techniques for observing the temperature structure of the atmosphere. *Bull. Amer. Meteor. Soc.*, **53**, 1074–1082.